IEEE Access
Multidisciplinary | Rapid Review | Open Access Journal

Received March 10, 2019, accepted April 8, 2019, date of publication April 11, 2019, date of current version April 24, 2019.

Digital Object Identifier 10.1109/ACCESS.2019.2910731

Single Cells of *Neurospora Crassa* Show Circadian Oscillations, Light Entrainment, Temperature Compensation, and Phase Synchronization

ZHAOJIE DENG[1], JIA HWEI CHEONG[1], CRISTIAN CARANICA[2], LINGYUN WU[3], XIAO QIU[4], MICHAEL T. JUDGE[5], BROOKE HULL[5], CARMEN RODRIGUEZ[5], JAMES GRIFFITH[5,6], AHMAD AL-OMARI[7], SAM ARSENAULT[1], HEINZ-BERND SCHÜTTLER[3], LEIDONG MAO[1], AND JONATHAN ARNOLD[5]

[1]School of Electrical and Computer Engineering, College of Engineering, University of Georgia, Athens, GA 30602, USA
[2]Department of Statistics, University of Georgia, Athens, GA 30602, USA
[3]Department of Physics and Astronomy, University of Georgia, Athens, GA 30602, USA
[4]Institute of Bioinformatics, University of Georgia, Athens, GA 30602, USA
[5]Genetics Department, University of Georgia, Athens, GA 30602, USA
[6]College of Agricultural and Environmental Sciences, University of Georgia, Athens, GA 30602, USA
[7]Department of Biomedical Systems and Informatics Engineering, Yarmouk University, Irbid 21163, Jordan

Corresponding authors: Leidong Mao (mao@uga.edu) and Jonathan Arnold (arnold@uga.edu)

This work was supported in part by the Joint Award MCB-SSB/PHY-POLS-1713746, one award being from the NSF Molecular and Cellular BioSciences [Systems and Synthetic Biology (SSB)] and the other award being from the NSF Physics of Living Systems (PoLS), and in part by the NSF Engineering Directorate under Grant ECCS-1150042.

ABSTRACT Using a microfluidics device, fluorescence of a recorder (mCherry or mVenus) gene driven by a *clock-controlled gene-2* promoter (*ccg-2p*) was measured simultaneously on over 1000 single cells of *Neurospora crassa* every half hour for 10 days under each of varied light and temperature conditions. Single cells were able to entrain to light over a wide range of day lengths, including 6, 12, or 36 h days. In addition, the period of oscillations in fluorescence remained remarkably stable over a physiological range of temperatures from 20 ^{o}C to 30 ^{o}C (Q_{10} = 1.00–1.07). These results provide evidence of an autonomous clock in most single cells of *N. crassa*. While most cells had clocks, there was substantial variation between clocks as measured by their phase, raising the question of how such cellular clocks in single cells phase-synchronize to achieve circadian behavior in eukaryotic systems at the macroscopic level of 10^7 cells, where most measurements on the clock are performed. Single cells were placed out of phase by allowing one population to receive 6 or 12 h more light before lights out (D/D). The average phase difference was reduced in the mixed population relative to two unmixed control populations.

INDEX TERMS Circadian rhythms, single cell measurements, single cell fluorescence, microfluidics, *Neurospora crassa*, light entrainment, temperature compensation, phase synchronization, ensemble methods, systems biology, biological clock, quorum sensing, stochastic resonance, gene regulatory networks, nonlinear dynamics, stochastic networks.

I. INTRODUCTION

The synchronization of the collective behavior of organisms can be observed in a variety of contexts [1], the blinking of fireflies, the collective marching of an army of locusts [2], the foraging of baboon troops [3], the schooling of fish, and the flocking of birds [4]. How this synchronization occurs remains a fundamental problem in biology. This synchronization occurs at other scales within organisms as well. Most organisms possess biological clocks [5], the ability to tell time so that an organism, eats, sleeps, or reproduces at the appropriate time, as examples. These biological clocks are observed at the level of 10^7 cells or more [6], where there is tight synchronization of the circadian rhythm between cells.

A fundamental question is how do circadian rhythms at the macroscopic scale of 10^7 cells originate at the single cell level. In a variety of systems, such as flies and mammals,

The associate editor coordinating the review of this manuscript and approving it for publication was Ho Ching Iu.

not all cells display circadian oscillations at the single cell level [7] in tissues, such as the mammalian suprachiasmatic nuclei (SCN) [8] or fly lateral neurons [9]. In both flies and mammals the presence of a few cells with circadian oscillations have been hypothesized to orchestrate the behavior of surrounding cells [10]. It is also possible that collective behavior, such as circadian rhythms, involves no leaders. For example, simple individual rules governing cells lead to aggregation behavior in the social amoeba, *Dictyostelium discoideum* [11]. In another example, collective movement of baboon troops does not appear to be governed by social hierarchy but by consensus decision making [3]. Thus, it is possible that circadian rhythms emerge from simple rules that connect the behavior of single cell oscillators to produce the properties of an entrainable circadian oscillator with temperature compensation.

Most studies have confined themselves to demonstrating circadian oscillations in single cells [8], [12] and have not examined the other two basic properties of a biological clock (with the exception of light entrainment in a synthetic system [13]), light entrainment and temperature compensation [5]. Temperature compensation here represents the ability to keep time when temperature fluctuates within physiological limits. While single cell measurements with yellow fluorescent protein have been used to show cell cycle gating of diurnal rhythms in the model cyanobacterium *Synechoccocus elongatus [14]*, both light entrainment *and* temperature compensation have only been demonstrated at the macroscopic level [15]. Demonstrating light entrainment at the single cell level is challenging in *S. elongatus* because transcription shuts down in the dark [16]. While single cell measurements with luciferase recorders have also been used to examine diurnal rhythms and temperature compensation in mammalian cell cultures [8], [17]–[19], there is a limited number of autonomous oscillators in the suprachiasmatic nuclei (SCN), whose clock-like properties are confounded by the presence of their neighbors [7]; moreover, the single cell rhythms dampen in the dark (D/D) when cells in culture are dispersed [17].

There are two classes of possible hypotheses about the origin of the biological clock at the macroscopic level of millions of cells. One hypothesis is that the clock is a property of single cells. Each cell has its own clock. Alternative hypotheses are that clock-like properties, such as diurnal rhythms, light entrainment, and temperature compensation are orchestrated by a few pacemaker cells [10] or are emergent properties of cell-to-cell synchronization. There also may be a positive role for stochastic intracellular noise in synchronizing single cell oscillators [17], [20], [21], whether or not single cells have clocks [22]. Here we begin to test these hypotheses in a model filamentous fungus, *Neurospora crassa*.

We developed a microfluidics platform (Fig. 1) that captured single cells of *Neurospora crassa* (*N. crassa*) to allow fluorescent measurements on a *mCherry* recorder driven by the *clock-controlled gene-2* (*ccg-2*) promoter [23] on over 1,000 isolated single cells simultaneously over ten days in a controlled temperature and light environment. In previous work we provided evidence that the viability of single cells remained at 80% +/- 2% over ten days and that single cells had circadian oscillations [24]. Here we provided evidence that most isolated cells in *N. crassa* had all three clock-like properties at the single cell level. While the clock-like behavior was found in individual cells, collective behavior of the cells needs further examination to understand how synchronization of stochastic clocks with different phases and amplitudes emerges from the stochastic intracellular noise (seen below) among these oscillators. The best video summary of this project can be found in the graphical abstract from the second paper in this series [25].

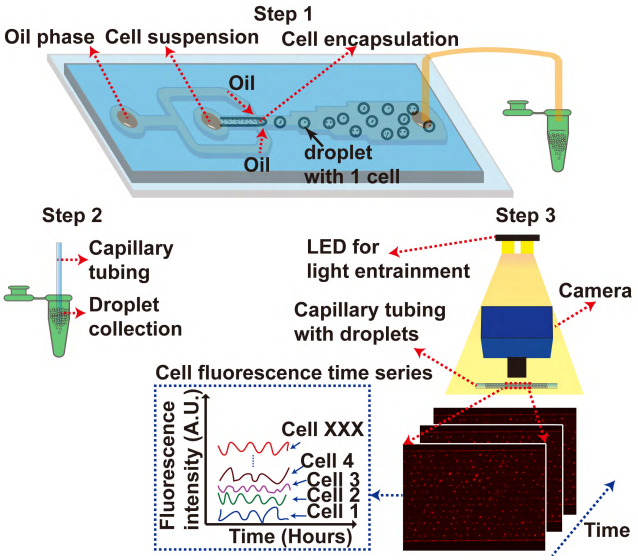

FIGURE 1. A microfluidic platform and its protocol enabled fluorescent measurements on a *mCherry* recorder driven by the *clock-controlled gene-2* (*ccg-2*) promoter on over 1,000 single cells simultaneously over ten days in a controlled temperature and light environment. In Step 1 of the protocol, encapsulation of *Neurospora crassa* cells into droplets was achieved via a flow-focusing droplet microfluidic device. The continuous phase was oil while the cells were suspended in aqueous media. The concentration of the cells was adjusted so that the majority of the droplets encapsulated just one cell. Droplets with encapsulated cells were collected into a vial. In Step 2, these droplets were transferred into a glass capillary tube for over ten days of fluorescent measurements. In Step 3, fluorescence of cells within the droplets and in the capillary tube were measured every 30 minutes. A LED light source was used for light entrainment, and the cells were kept at a set temperature throughput the measurement. Time series of fluorescent measurement over ten days (10 x 24 h) of single cells were obtained as a result.

II. MATERIALS AND METHODS

A. STRAINS, GROWTH, AND MODEL FITTING

As a control for the light entrainment experiments, the double knockout, *bd, ccg-2P:mCherry,wc-1*^{KO}, *frq*^{KO} was generated from two crosses. First, a *bd,ccg-2P:mCherry,A [26]* was crossed to *wc-1*$^{KO[27]}$(Fungal Genetics Stock Center (FGSC) 11711) to produce *bd,ccg-2P:mCherry,wc-1*^{KO}*A (wc-145)*. Then progeny of this cross were crossed to *ccg-2P:mCherry*, *frq*$^{KO[24]}$ (*frq51* [26]) generated from a cross, MFNC9 x FGSC 15070 [26] to obtain a fluorescent double knockout.

TABLE 1. Global response (R) and Kuramoto order parameter (K) of single cells as a function of day length. The standard errors (SE) were computed by bootstrap resampling of single cells. The bootstrap sample size used was 1,000.

	DD	6 hour artificial day (L/D)	12 hour artificial day (L/D)	36 hour artificial day (L/D)
R (+/- 2SE)	0.0696 (+/- 0.0915)	8.1869 (+/- 1.0338)	56.7945 (+/- 4.1433)	29.0865 (+/- 2.4654)
K (+/- 2SE)	0.0798 (+/- 0.0026)	0.3013 (+/- 0.0066)	0.4212 (+/- 0.0076)	0.3277 (+/- 0.0069)

The identification of the double knockout employed a hygromycin screen (.2 mg/ml), then a race tube screen (.1% glucose + Vogels media), followed by a fluorescent screen [26], and finally a PCR screen using *wc-1* and *frq* WT primers (S Table 1), in that order. The double knockout grown on slants displayed the characteristic aconidial white ring at 34 ^{0}C [28].

Cells with an *mCherry* recorder engineered to a *ccg-2* promoter [23] were first placed under a LED light source (color temperature 6500K) for 26 h in media described previously [24]. Cells were isolated with a flow-focusing geometry of a polydimethylsiloxane (PDMS) microfluidics device (Fig. 1). Cells were immobilized in a capillary tube with 50 micron depth and observed under a Zeiss Microscope Axio Imager.A2 at 5X over 10 days on a Zeiss motorized thermal stage (Mechanical stage 75 x 50 R). For the light entrainment experiments the same LED light source was utilized (5300 lux). The filter set was for excitation at 588/27 with emission at LP 615 (Zeiss #60HE) [29]. The excitation spectrum is given at https://www.micro-shop.zeiss.com/index.php?s=1502076664024ba&l=en&p=de&f=f&a=v&b=f&id=489060-9901-000&o=.

A universal system of measurement of fluorescent time series on each cell was utilized [24], in which the stochastic intracellular noise was separated from the detection noise with a parallel fluorescent bead experiment, in which fluorescent beads were substituted for living cells. A Matlab routine was developed to track individual cells over time [24]. Each fluorescent time series were normalized with Rhodamine B, detrended, and the periodogram computed [24]. The resulting periodogram was bias-corrected [24].

Then two models, a fully stochastic model [30] and mostly deterministic hybrid model with transcriptional bursting in *ccg-2* and *frq* were fit by Markov Chain Monte Carlo to the bias-corrected periodogram [24], [31] with a graphical summary in the Results.

B. CALCULATING PHASE

The discrete Hilbert phase $F^H(t)$ was computed from the Hilbert transform of the time series x(t) by $\tilde{x}(t) = PV\frac{1}{\pi}\int_{-\infty}^{\infty}\frac{x(\tau)}{t-\tau}d\tau$, where the integral is understood as taken in the principal value (PV) sense. The Hilbert transform $\tilde{x}(t)$ was computed from the Fast Fourier Transform [32]. The Hilbert phase is defined as a phase angle $F^H(t) = tan^{-1}(\frac{\tilde{x}(t)}{x(t)})$ [33]. The phase is defined from the continuized Hilbert Phase $F^C(t)$ by the relation: $M^C = \left|F^C(t_1) - F^C(t_0)\right|/2\pi$ in units of cycles. This phase changes with the time interval considered. To avoid jumps in the discrete Hilbert phase, the continuized Hilbert phase is defined recursively by $F^C(t+1) = F^C(t) + m^C(t)\,2\pi$, where the argument $m = m^C(t)$ minimizes $Df_m = \left|F^H(t+1) - F^H(t) + 2\pi m\right|$. A fuller explication of this phase calculation is given in results along with a graphical summary of phase measures in the Results.

C. THE PCCG-2:MVENUS FLUORESCENT STRAIN WAS ENGINEERED BY CRISPR/CAS9 IN N. CRASSA

In order to carry out the mixing experiment with two populations of cells with different phases, a second fluorescent recorder construct was needed with non-overlapping excitation and emission spectra to mCherry. The mVenus fluorescent recorder was recommended [34]. An M249 plasmid served as the starting point [35] (with construct strategy in supplementary S Fig. 1); this plasmid (S Fig. 2) contained a bialaphos selectable marker for transformation of *N. crassa* as well as a luciferase recorder. A pUC57 plasmid containing *Pccg-2:mVenus* was generated (Genscript, Inc., 860 Centennial Ave, Pascataway, NJ 08854) with homology to M249. The gsy:luc segment in M249 was replaced at the BstB1 and SgrDI restriction sites in M249 with the *Pccg-2:mVenus* fragment. The M249 with *Pccg-2:mVenus* was co-transformed with a plasmid encoding Cas9 (p415-GalL-Cas9-CYC1t) and with the *csr-1* specific guide RNA (p426-SNR52p-gRNA.CAN1.Y-SUP4t) [35] by electroporation. Electroporation into *N. crassa* was done with a Genepulser Xcell electroporater set at 7.5 kV/cm (1.5 kV in a 2cm cuvette), capacitance of 25 mF, and resistance of 600 ohms (BioRad, Hercules, CA). A more detailed description of the mVenus recorder construct in *N. crassa* is available [29]. The strain was made homokaryotic with a cross to a *band*(*bd*) strain(1858A, Fungal Genetics Stock Center, Manhattan, KS). The mCherry and mVenus recorder strains were grown in media as above and placed in a LED light source as described in Fig. 8A to convert the mVenus strains to night owls. The filter set for excitation of mCherry (mVenus) was at 585/35 (478/28) with emission at 645/60 (527/54) (Zeiss #61HE) [29]. The excitation spectrum is given at: https://www.micro-shop.zeiss.com/index.php?s=1502076664024ba&l=en&p=de&f=f&a=v&b=f&id=489061-9901-000&o=

The remaining part of the mixture experiment is summarized in Results.

The data sets generated during the current study are available from the corresponding authors on reasonable request

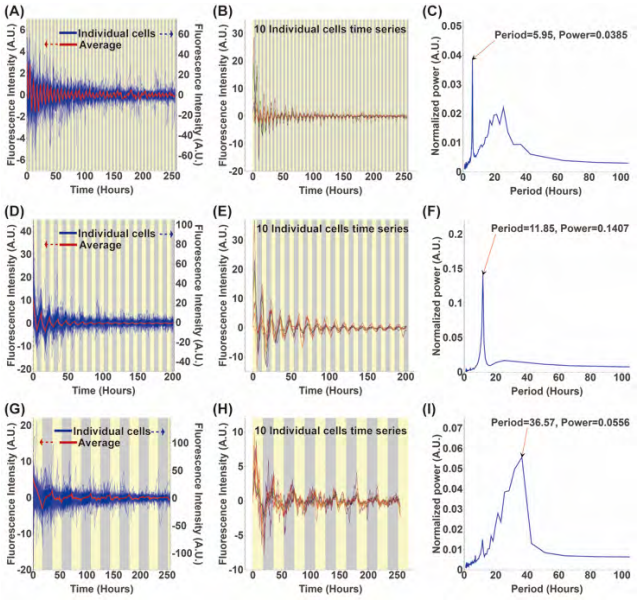

FIGURE 2. Single cells of *N. crassa* entrained to a 6 hour (A-C), 12 hour (D-F), and 36 hour day (G-I). (A) Single cell trajectories (Rhodamine B normalized and detrended) under varied L/D regimens. (B) Ten randomly sampled trajectories (Rhodamine B normalized and detrended) displayed synchronization. (C) Average periodogram of > 1, 000 cells over ten days (10 × 24 h) for three days of different length (6, 12, and 18 h day length). Yellow denotes light (L), and grey denotes dark (D).

and at DOI: 10.21227/72gy-xb81 in the IEEEDataPort under the title of this work.

III. RESULTS

A. SINGLE CELLS ENTRAIN TO LIGHT FOR A 6, 12, OR 36 H DAY

A light signal at the macroscopic scale served to entrain a circadian oscillator to a six hour day or a 36 hour day [36], [37] (L/D) with equal periods of light (L) and dark (D) for the model system, *N. crassa*. The question remains whether or not such a clock property exists at the single cell level. Recently light entrainment studies at the single cell level have included a small number of cells in Zebrafish [38], tracking of cells (not isolated) in the SCN of mice [19], tracking ∼100 single cells (not isolated) in tissue of the duckweed, *Lemna gibba* [39], and tracking ∼100 single cells (not isolated) in tissue of *Arabidopsis thaliana* [40]. The limitations of the mice and duckweed studies, as examples, are that single cells were not isolated to distinguish whether or not light entrainment is a single cell property. Not only did we wish to test whether light entrainment occurs in single cells, we wanted to know whether single cells would track a L/D cycle over very short or very long days [19]. There might be a light period sufficiently far from the intrinsic period of cells in the dark of 21 h [24], at which light entrainment fails.

In Fig. 2 is shown the light entrainment of single cells of *N. crassa* for 6 hour, 12 hour, and 36 hour days. In spite of the substantial variation between >1,000 trajectories of *ccg-2* expression in Fig. 2A (of which less than 6% is detection noise [24]), sampling ten trajectories in Fig. 2B under the light(L)/dark(D) regime showed the trajectories oscillating with night (grey) and day (yellow). The trajectories were seen to synchronize in Fig. 2B, 2E, and 2H to the L/D cycle of the light source for all three day lengths (even in the average trajectories in Fig. 2A). A standard way to examine the periodicity of the fluorescent series is the periodogram or power spectrum [24]. In Fig. 2C, 2F, and 2I all three average (over cells) periodograms for >1,000 cells for each day were remarkably consistent with the period of the light source (6, 12, or 36 h). The only difference is that the variation in synchronization appeared larger in the 36 h light source (Fig. 2H). This variation was also reflected in the tightness of the periodogram about the frequency of the driving light signal. Over a wide range in period (6-36 h) of the driving signal the cells with an intrinsic period of 21 h were able to entrain to the external driver.

The data in Fig. 2 can be used to test the whether or not each cell has a clock against the alternative that only some cells have clocks serving as pacemakers for the rest of the cells [10]. The test is simply to sample repeatedly another collection of 10 isolated cells and compute their Rhodamine B normalized and detrended trajectories and periodograms averaged over 10 cells, a procedure known as the bootstrap [41]. If each cell has its own clock, then Fig.s 2 B, E, H, C, F, and I will not change much from collection to collection. If only some pacemaker cells have a clock, then some collections without a pacemaker will look very different with respect to trajectories and periodograms. This experiment was done (S Fig. 3) for 1,000 collections of size 10, and all of the groups had the same highly synchronous behavior. For example, the 95% confidence bands closely track the mean fluorescence over 1,000 10-cell collections, thus providing direct evidence that cells have their own clocks, and the 10-cell average periodograms entrain to the L/D cycle of the 6, 12, and 36 h days.

B. LIGHT DRIVEN SINGLE CELL OSCILLATORS DO SHOW SUBSTANTIAL VARIATION IN PERIOD, AMPLITUDE, AND PHASE BETWEEN CELLS

It would be desirable to know the kind and cause of variation displayed among oscillators that entrain to light. The reason is that stochastic intracellular noise can have functional consequences for the cell, affecting genetic switches [42], coordinated regulation [43] as in clock-controlled genes, and combinatorial regulation [44]. In particular, it can affect the synchronization of stochastic clocks [17], [22]. Each driven cell oscillator has a characteristic period, amplitude, and phase. In the dark (D/D) it was argued in previous work [24] that period and amplitude should be positively correlated as related features in the periodogram; likewise, we hypothesized there should be an inverse relation between phase (i.e., the number of cycles completed in a fixed period of time) and period [24] because phase defined below is counting cycles completed in a fixed period of time. If the period were longer, the expectation is that fewer cycles would be

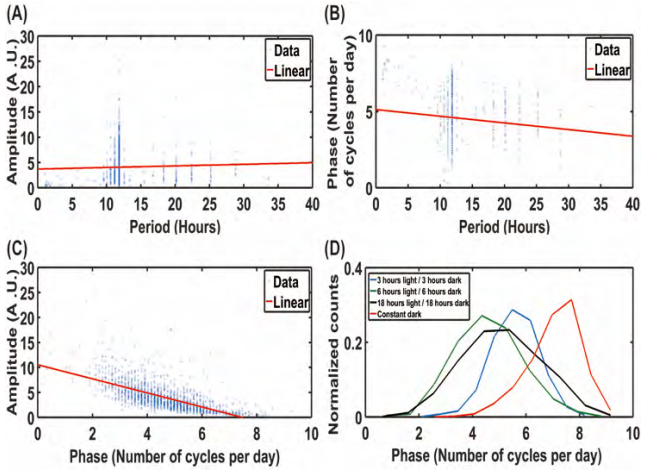

FIGURE 3. Period, amplitude and phase of 1,626 entrained oscillators under 6 hours light on and 6 hours light off. (A) Amplitude vs. period of 1,626 single cell oscillators in Figure 2.D. The amplitude is half of the square root of the maximum power in the periodogram of each cell; the period occurs at the maximum in the periodogram of individual cells. The correlation (r) of amplitude and period was $r = 0.0358$ (Fishers $z = 0.0359$, $P = 0.1485$) [53]. The Spearman rank correlation (r_s) was $r_s = 0.0935$ ($P = 0.0002$) [54]. The straight line regression of amplitude on period is shown in red. (B) Plot of phase vs. period of 1626 single cell oscillators in Fig. 2.D. The phase as derived from the Hilbert transform is defined previously [24], and a full description of its computation is given in the Materials and Methods. The units of phase graphed are cycles per 24 h (*i.e.*, per day). The correlation (r) of phase and period was $r = -0.1079$ (Fishers $z = -0.1083$, $P < 0.001$) [53]. The Spearman rank correlation (r_s) was $r_s = -0.0406$ ($P < 0.001$) [54]. The straight line regression of phase on period is shown in red. (C) Plot of amplitude vs. phase for 1626 single cell oscillators in Fig. 2D. The correlation (r) of amplitude and phase was $r = -0.6543$ (Fishers $z = -0.7829$, $P < 0.001$) [53]. The Spearman rank correlation (r_s) was $r_s = -0.7409$ ($P < 0.001$) [54]. The straight line regression of phase on period is shown in red. (D) Phase histograms of > 1,000 single cell oscillators under varied light conditions. The mean phase (+/− two standard errors), for example, of the entrained oscillators under a 12 h day was 4.5816 (+/ − 0.0626) cycles per day (24 h). The mean phase for a 6 h day was 5.5868 (+/ − 0.0485). The mean phase for a 36 h day was 5.1177(+/ − 0.0656).

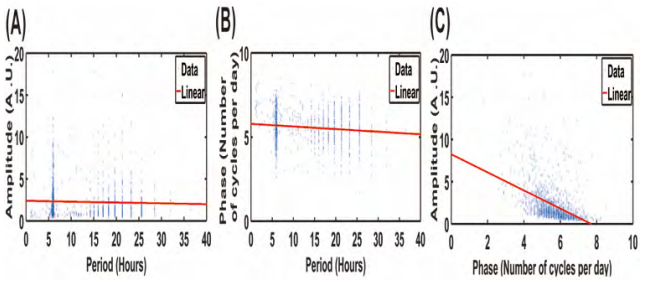

FIGURE 4. Period, amplitude and phase of 1,330 entrained oscillators under 3 hours light on and 3 hours light off. (A) Amplitude vs. period of 1,330 single cell oscillators in Fig. 2A. The amplitude is half of the square root of the maximum power in the periodogram of each cell; the period occurs at the maximum in the periodogram of individual cells. The correlation (r) of amplitude and period was $r = -0.035$ (Fishers $z = -0.035$, $P = 0.2016$) [53]. The Spearman rank correlation (r_s) was $r_s = -0.057$ ($P = 0.0378$) [54]. The straight line regression of amplitude on period is shown in red. (B) Plot of phase vs. period of 1,330 single cell oscillators in Fig. 2A. The phase is defined as described previously [24] (also see Materials and Methods) but also normalized by dividing by the number of days (with 24 h per day) of the measurement. The correlation (r) of phase and period was $r = -0.1373$ (Fishers $z = -0.1382$, $P < 0.001$) [53]. The Spearman rank correlation (r_s) was $r_s = -0.1221$ ($P < 0.001$) [54]. The straight line regression of phase on period is shown in red. (C) Plot of amplitude vs. phase for 1330 single cell oscillators in Fig. 2A. The correlation (r) of amplitude and phase was $r = -0.4310$ (Fishers $z = -0.4612$, $P < 0.001$) [53]. The Spearman rank correlation (r_s) was $r_s = -0.5644$ ($P < 0.001$) [54]. The straight line regression of phase on period is shown in red.

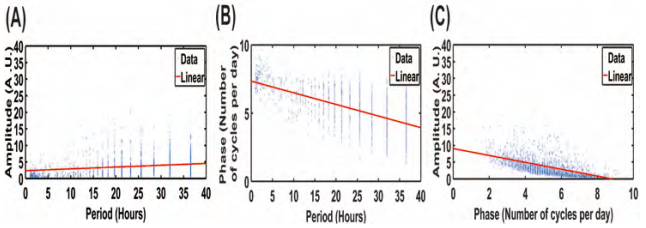

FIGURE 5. Period, amplitude and phase of the 1,969 entrained oscillators under 18 hours light on and 18 hours light off. (A) Amplitude vs. period of 1,969 single cell oscillators in Fig. 2G. The amplitude is half of the square root of the maximum power in the periodogram of each cell; the period occurs at the maximum of the periodogram of single cells. The phase is defined as described previously [24] (also see Materials and Methods) but also normalized by dividing by the number of days (each day having 24 h) of the measurement. The correlation (r) of amplitude and period was $r = 0.1852$ (Fishers $z = 0.1873$, $P < 0.001$) [53]. The Spearman rank correlation (r_s) was $r_s = 0.2843$ ($P < 0.001$) [54]. The straight line regression of amplitude on period is shown in red. (B) Plot of phase vs. period of 1969 single cell oscillators in Fig. 2.G. The phase is defined as described previously [24] but also normalized by dividing by the number of days of the measurement. The correlation (r) of phase and period was $r = -0.6248$ (Fishers $z = -0.7328$, $P < 0.001$) [53]. The Spearman rank correlation (r_s) was $r_s = -0.5600$ ($P < 0.001$) [54]. The straight line regression of phase on period is shown in red. (C) Plot of amplitude vs. phase for 1,969 single cell oscillators in Fig. 2G. The correlation (r) of amplitude and phase was $r = -0.4752$ (Fishers $z = -0.5168$, $P < 0.001$) [53]. The Spearman rank correlation (r_s) was $r_s = -0.6510$ ($P < 0.001$) [54]. The straight line regression of phase on period is shown in red.

completed. These relationships among period, amplitude, and phase are also important because they provide insights into models for the clock [45], [46]. In a 12 h and 36 h day the expectation was met. Only in the 6 h day was there a slightly negative correlation between amplitude and period (Fig. 3-5). The notion of phase used here (and defined in Materials and Methods), the number of cycles completed in a fixed period of time was introduced over 300 years ago [47], [48] in the description of coupled pendula, and its computation from the Hilbert transform was introduced in the early Twentieth Century [49]. This notion of phase has been used both in a physical context [33] and in a biological context [50], [51] down to the present. There are several advantages of the phase used here. The phase is functionally independent of period and amplitude, thus providing new information about oscillations [24]. The phase can be calculated in an integrated way with the periods, amplitudes, and phases of the system using the Fast Fourier Transform [33] as described in the Materials and Methods. The phase measure used here changes with time, as in the data here.

The simplest notion of phase arises in a periodic process described by the sinusoid $x(t) = A\cos(\omega t + \phi)$ for all times t, where x(t) is the fluorescent series for a single cell. The quantity A is the amplitude, ω, the frequency, and ϕ, the phase shift. If the series were sinusoidal for all time, then

the phase shift ϕ would capture all of the phase information about a single cell. The sinusoid x(t) = $Acos(\omega t + \phi)$ could be fitted to the fluorescent series on each cells (as in S Fig. 4) to summarize the phase variation across cells.

Unfortunately the phase changed nonlinearly over time (see below). To capture the time variation in the phase a replica $\tilde{x}(t)$ was created of the original process x(t) as described in the Materials and Methods. This replica $\tilde{x}(t)$ (known as the Hilbert Transform) was 90^0 [26] out of phase with the original process x(t). For example, if the original process were x(t) = $cos(\omega t)$, then the replica would be $\tilde{x}(t) = sin(\omega t)$. The Hilbert phase $F^H(t)$ is defined as the phase angle between the original process x(t) and the replica $\tilde{x}(t)$, namely

$$F^H(t) = tan^{-1}\left(\frac{\tilde{x}(t)}{x(t)}\right).$$

This Hilbert phase takes values between $-\pi$ and π. As an example if the process were x(t) = $cos(\omega t + \phi)$, then the Hilbert phase would be simply $F^H(t) = tan^{-1}\left(\frac{\tilde{x}(t)}{x(t)}\right) = \omega t + \phi$. This phase angle increases linearly with time for a sinusoid with slope ω and y-intercept as the phase shift ϕ. Phase differences at time 0 could then be extrapolated to phase differences at time 10, 24 h days later. In contrast, the Hilbert phase was nonlinear for the fluorescent series considered here (see below), and the design of the experiments was chosen to synchronize cells at the beginning of an experiment by exposing cells to 26 h of light initially (see Materials and Methods), thereby making the phase shifts between cells small initially.

Fortunately it is not necessary to assume that a cell's fluorescent series x(t) is sinusoidal, and the Hilbert phase can still be calculated for each cell over time (see Materials and Methods) under very general assumptions. The Hilbert phase, however, will experience discontinuities at $-\pi$ and π, and to avoid these discontinuities the Hilbert Phase $F^H(t)$ was used to construct a continuized Hilbert phase $F^C(t)$ as described in Materials and Methods, like the smooth Hilbert phase $\omega t + \phi$ of the sinusoid, but without assuming linearity.

It is useful to think of each cell's Hilbert phase being captured by a complex number, $(x(t), \tilde{x}(t))$, where x(t) is the real part and $\tilde{x}(t)$ is the imaginary part. For a periodic process, as the phase angle $F^H(t)$ sweeps between $-\pi$ and π, then this curve $(x(t), \tilde{x}(t))$ in the complex plane describes a cycle about its origin (0, 0). The phase M^C can be thought of as the number of cycles completed by the process in the complex plane between time t_0 and time t_1. Phase is usually measured in terms of the number of cycles completed (obtained by dividing by 2π), and the ancillary annoyance of the phase shift at time zero is subtracted out to yield the phase:

$$M^C(t_1, t_0) = \left[F^C(t_1) - F^C(t_0)\right]/2\pi$$

A complete graphical summary of all 4 phase measures $(\phi, F^H(t), F^C(t) and\ M^C)$ is given below. This phase is plotted in Figures 3-5. In these plots the phase was evaluated

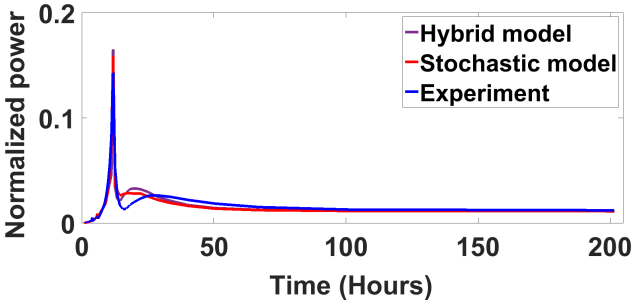

FIGURE 6. Two stochastic models explained the single cell light entrainment data. A hybrid stochastic network with only transcriptional bursting in *frq* and *ccg-2* gene explained the periodogram of single cells from the light entrainment experiment using data on 6 h light and 6 h dark. The remaining part of the network is deterministic and described elsewhere [24]. The hybrid largely deterministic model was fit by Markov Chain Monte Carlo to the periodogram [59] using a Metropolis-Hastings updating rule. The final minimum chi-squared statistic $\mathcal{X}^2$ was 1246.9 after 1000 sweeps. The second model is a full stochastic model [30]. The full stochastic model was fit by Markov Chain Monte Carlo to the periodogram using parallel tempering [30]. The final minimum chi-squared statistic $\mathcal{X}^2$ was 1003.56.

for t_1 = 10, 24 h days and t_0 = 0. If the phase and Hilbert Phase are considered as a function of time t_1, then the time evolution of phase of single cells can be observed as well to see how phase synchronization between cells arises (see below).

Understanding ultimately where the variation in phase, amplitude, and period originates (Fig. 3-5) has involved the development of stochastic networks for the clock [30]. Established and well understood methods for fitting these models involved the use of the periodogram or "power spectrum", which captured the period and amplitude information [30], [31]. In that the phase defined here is functionally independent of the periodogram [24], the phase can provide an independent test of the fit of the model and has been so used for the clock network [30]. One of the fundamental features of networks identified at the single cell level is that most of the variation in the fluorescent observations (as summarized in Fig. 3-5) on macromolecules arises from stochastic intracellular variation in the cell as opposed to detection noise [24]. That still leaves open the question of whether this variation arises at the genic, transcriptional, or translational level as examples. A combination of new experiments and models may help us to address this question.

The source of this variation is explainable by stochastic intracellular variation arising from a stochastic network proposed earlier [24] – this stochastic network explained quite well the periodogram of a 12 h day (Fig. 6). A simpler largely deterministic (hybrid) model with only stochastic gene activation of *ccg-2* and the *frequency* (*frq*) oscillator explained much of the variation in the periodogram as well (Fig. 6). The deterministic negative feedback model falls in the class of Hill Type transcriptional repression models [52]. While there was variation in all three descriptors of single cell oscillators, it is clear there was substantial variation in phase between single cell oscillators driven by light (Fig. 3D), but this variation

for all three entrainment experiments was much less than for D/D experiments [24]. This could be explained if light acts to synchronize the cells.

There has been some speculation that single cell oscillators with larger amplitude would be less likely to entrain to light and be more robust in their intrinsic period [19]. The best candidates are the single cell oscillators in Fig. 4, in which there is a collection of entrainable oscillators at ∼6 h and another group at ∼24 h in Fig. 2C. Based on Fig. 4C the oscillators were split into a group with amplitude > 7 a. u. and another group with amplitude ≤7 a. u. The split of 7 a. u. was selected from Fig. 4C independently of the oscillator period to insure a large number of oscillators above and below the amplitude cutoff. The probability of the large amplitude group at the 21 h period is higher than the small amplitude group at the 25.6 h period. This difference in the normalized periodograms in S Fig. 5-6 for the two groups of oscillators was significant by a Kolmogorov-Smirnov (KS) test at $P < 0.001$ [54]. The large amplitude group also seemed more robust with respect to the intrinsic rhythm of 21 h in S Fig. 5. The same phenomenon has been reported for the *period* gene in mammalian systems [55]. A *Clock* mutation (homolog to *wc-1*) converts a WT strain with large amplitudes in the *Period* gene (homolog to *frq*) normally resistant to light entrainment into a smaller amplitude *Period* gene which is now entrainable. While the KS test is nonparametric, the caveat is that it may not capture the stochastic intracellular variation in the period from cell to cell [30]. On the other hand, most of the variation in Fig.s 3-5 is in phase, not in period, which is being examined in the KS test in S Fig. 5-6.

There were three controls used in the light entrainment experiments: (1) use of Rhodamine B in each light entrainment experiment to examine the effects on a chromophore independently of the clock; (2) use of a knockout strain containing mCherry (*ccg-2P:mCher*ry) with a double knockout of the *white-collar-1*(*wc-1)*, the light receptor and positive element of the *N. crassa* FRQ-based clock system and the negative element in the clock, *frequency* (*frq*) gene (see Materials and Methods); (3) use of a relaxation experiment in which cells in a L/D experiment were shifted to a D/D experiment to see if the cells return to their intrinsic period of 21 h in the dark (D/D). In the former control Rhodamine B fluorescence was observed in parallel with the fluorescent measurements on all cells in Fig. 3-5 to remove uncontrolled periodic and aperiodic factors by Rhodamine B normalization (see Materials and Methods). The intensity of the Rhodamine B signal was typically ∼2,000 a.u. while the intensity of fluorescence in living cells was typically two orders of magnitude larger at ∼94,000 a.u. The periodograms for each of these Rhodamine B time series are in S Fig. 7. These periodograms had a maximum in their residual variation, which did not track the entrainment period in each of the experiments in Fig. 3-5.

In the second control a light entrainment experiment with 12 h day (Fig. 4) was performed on *ccg-2P:mCherry,bd,wc-1*^{KO}, *frq*^{KO} (see Materials and Methods). Again the major component of the periodogram of the double knockout did not track to 12 h, as did the strain without the knockouts (S Fig. 8). There was a secondary peak consistent with an earlier finding of a single knockout in *frq* not totally obliterating the clock [24] under D/D conditions or the clock in *S. elongatus [56]*. As hypothesized earlier [24], this secondary peak could be explained by a secondary FRQ-less clock that is orchestrating light entrainment as well or alternatively, the FRQ-based oscillator is secondary. Neither hypothesis can be excluded at this stage. Entrainment studies at the macroscopic scale have been used to argue for [57] and against [58] such a FRQ-less clock using race tube experiments.

In the last control, the cells were shifted from a L/D regime of a 12 hour day as in Fig. 3 for 4, 24 h, days to a D/D regime for 4, 24 h days. Under light entrainment the expectation is that the cellular oscillators would relax from a driven period of 12 h to an intrinsic period in the dark of 21 h. That is exactly what was observed in S Fig. 9. Under the L/D regime the period was 12 h, and under the D/D regime the period was 21 h as expected [24].

C. LIGHT SYNCHRONIZES SINGLE CELLS

The synchronization of single cells by light in distinct non-communicating droplets can be measured in a variety of ways [60]. A standard way is the Kuramoto order parameter (K) [60], [61]:

$$k = \langle \left| \langle n^{-1} \sum_{j=1}^{n} \exp\left(i\mathrm{M}_j\right) - \langle n^{-1} \sum_{j=1}^{n} \exp\left(i\mathrm{M}_j\right) \rangle \right| \rangle,$$

where n is the number of single cells or ''singletons'' and the phase introduced earlier is denoted by M_j, that is the phase (Fig. 3) for the jth cell as defined in the Materials and Methods. The brackets $\langle\ \rangle$ denote a time average over the argument. The quantity K approaches 1 as all cells approach perfect synchronization and approaches zero as all cells oscillate out of phase with each other. In the dark (D/D) the singletons showed less synchrony (∼0.08 in Table 1), but the cells exposed to a periodic driving signal showed a high degree of synchronization with the light signal (Table 1). In support of each cell having a clock, also the bootstrap samples with 10 cells each had a mean of the Kuramoto K across 1,000 bootstrap samples of $0.5022 + / 1.0013$ similar to Table 1. There also appeared to be an intermediate optimum for synchronization with, for example, the synchronization being lower for the 36 h day or 6 h day.

D. THE LIGHT RESPONSE OF CELLS RESONATES WITH THE LIGHT SIGNAL

Pittendrigh argued that the intrinsic rhythm of the biological clock of an organism resonated with the light cycle experienced by the organism [62]. To demonstrate this resonance we utilized a measure of the strength of the entrainment

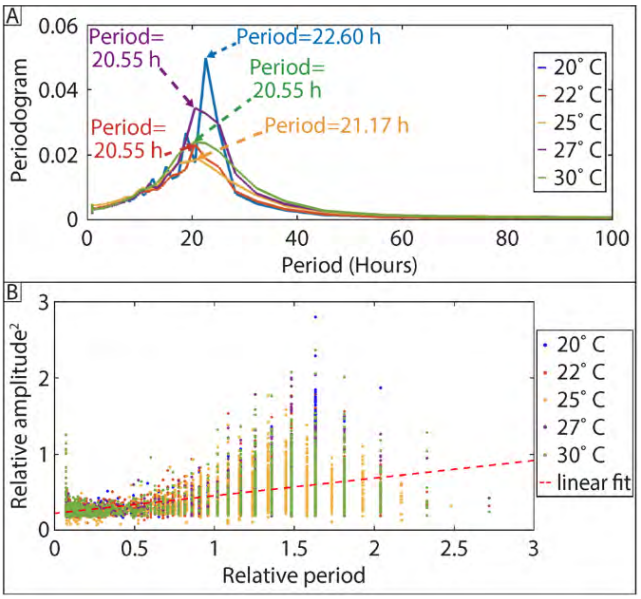

FIGURE 7. Oscillators in single cells displayed temperature compensation. (A) The average normalized periodogram at each of five temperatures over the physiological range of the organism is shown. Each average normalized periodogram at each temperature is based on over 1,000 isolated cells. (B)The coupling of the relative amplitude squared (from the maximum in each single cell periodogram) is plotted vs. relative period. The amplitude squared and period of each single cell oscillator is divided by the average amplitude squared and period at 30 ^{0}C over all cells at 30 ^{0}C to produce the relative amplitude squared and relative period. Single cells are color coded for temperature as in panel A. The correlation (r) of amplitude squared and period was r = 0.4830 (Fishers z = 0.5269, P < 0.0001) [53]. The Spearman rank correlation (r_S) was r_S = 0.5599 (P < 0.0001) [54].

response (R) to variation in the length of the day [63]:

$$R = \frac{4}{L_0^2}\left|\left\langle \exp\left(-i\omega t\right)\frac{1}{n}\sum_{j=1}^{n} X_j\right\rangle\right|,$$

where L_o is the external light intensity (5300 lux), ω is the driving frequency of the 6, 12, or 36 hour day (Fig. 2), and X_j is the fluorescent intensity of the j-th cell. This response R can also be interpreted as the absolute magnitude of the Fourier coefficient of the average fluorescence over n cells at the driving frequency ω and normalized by the square of the light intensity (L_0). As can be seen in Table 1, there was an intermediate optimum in the entrainment response to variation in the day length, suggesting resonance with the intrinsic frequency of the circadian oscillator.

E. SINGLE CELLS DISPLAY TEMPERATURE COMPENSATION

One of the fundamental properties of the biological clock is temperature compensation [64], that is robustness of the clock period over a physiological range of temperatures for the organism. Here we provided evidence that single cells have this property (Fig. 7). As the temperature varies over the range of 20-30 ^{o}C, the periods derived from the periodograms in Fig. 7A fluctuated little. This was quantified by the Q_{10} measure:

TABLE 2. Temperature coefficient Q_{10} over a physiological range of temperatures (T_1) provided evidence of temperature compensation. Standard errors (SE) were computed as in Table 1.

Temperature(T_1)	20 ^{o}C	22 ^{o}C	25 ^{o}C	27 ^{o}C
Period(Hours) (+/- 2SE)	22.2497 (+/- 2.1879)	20.6643 (+/- 1.0972)	20.7932 (+/- 1.6384)	20.7000 (+/- 1.1047)
Q_{10} (+/- 2SE)	1.0757 (+/- 0.1231)	0.9991 (+/- 0.0822)	1.0053 (+/- 0.1005)	1.0008 (+/- 0.0822)

$$Q_{10} = \left(\frac{P_1}{P_2}\right)^{\frac{10}{T_1 - T_2}},$$

which measures the rate of change of the period (P) over 10 ^{o}C. The reference temperature (T_2) was 30 ^{o}C. The Q_{10} values were at or near 1, indicating little change in period with temperature (Table 2). Incidentally the temperature compensation data (Fig. 7A) reaffirmed the diurnal oscillations needed for demonstrating a biological clock found earlier [24]. With the entrainment experiment and temperature experiment we conclude that single cells of *N. crassa* have a biological clock.

It would be desirable to know the mechanism of temperature compensation from the data in Fig. 7A. Several classes of clock models are predicted to have amplitude-period coupling when these models display temperature compensation [45]. We examined the coupling of relative amplitude to relative period in Fig. 7B in over 4,000 single cell oscillators. The highly significant positive slope (P < 0.0001) of relative amplitude squared on relative period was consistent with that predicted by three families of clock models including one of with a model with both positive and negative feedback loops [45], as in the working model for the *N. crassa* clock [59].

Recently a very interesting phosphoswitch model was proposed to explain temperature compensation in mice [65]. There are two phosphorylation sites on PERIOD2, the homolog of *FRQ*, which act as a switch between two degradation pathways for the oscillator protein, one with exponential decay and one with a more complicated three stage degradation. If such a switch were operating on FRQ, then the rising and falling phase might be different at different temperatures. To unpack the phase differences at different temperatures, the phase curves were calculated at two extreme temperatures (S Fig. 10). The phase curves at the extreme temperatures of 20 ^{0}C and 30 ^{0}C steadily diverged in time (see S Fig. 10). These results suggest a reexamination of the phosphoswitch hypothesis for FRQ as an alternative to the temperature compensation mechanism based on alternative translation initiation of *frq* [66], [67].

While we have provided evidence that single cells do have a clock (Fig. 2 and 7A), an open question remains – how does the clock originate at the macroscopic level by

overcoming the stochastic intracellular noise from cell to cell (Fig. 3)? There could be a variety of mechanisms (Fig. 6) at work including a positive role for noise in synchronization of individual cells [20], [30]. The synchronization of single cell oscillators in tissues is hypothesized to have roles in disease [68], [69] and aging [5].

F. CELLULAR CLOCKS COMMUNICATE PHASE

We have provided evidence that single cells have autonomous biological clocks in *N. crassa*. This conclusion narrows the field of hypotheses explaining how single cell oscillators give rise to synchronized behavior at the macroscopic level. It is unnecessary to postulate clock properties, such as light entrainment and temperature compensation, are emergent properties of single cell clocks; moreover, in Fig 2 and S Fig. 3 there was positive evidence that single cells had clocks as opposed to a few cells acting as pacemakers [10]. In Fig.s 3-5 there was less variation in amplitude and period and substantial variation in phase (Fig. 3D). For example, in Fig. 3C there was substantial variation in phase, but little variation in amplitude. In Fig. 3B there was substantial variation in phase, but a concentration of single cell clocks at the period of the light source. These results were found as the day length was varied (Fig. 4-5). This observation limits the range of hypotheses to those explaining phase synchronization between single cell clocks.

In previous work Deng *et al.* [24] presented indirect evidence for cell-to-cell communication – cells in the same droplet tended to synchronize in the dark, and the degree of synchronization increased with the number of cells per droplet as expected under quorum sensing. Also, there was evidence that in a flow-through reactor *N. crassa* may lose a chemical signal(s) needed for clock synchronization [70]. In Fig. 8 evidence for phase synchronization by mixing two cell populations (larks and night owls) that are completely out of phase was presented. This phase synchronization is a prediction of a quorum sensing mechanism detailed previously [24] (see supplementary video). We constructed one cell population containing an mCherry recorder under *ccg-2p* control at the *his-3* locus [23] and another population, containing an mVenus recorder under *ccg-2p* promoter control engineered at the *csr-1* locus using CRISPR/Cas9 (see Materials and Methods) [35].

Each population was phase-synchronized with 2 hours of light initially, and the mCherry population was phase-shifted by 12 hours of additional light (night owls) relative to mVenus (larks) (See Fig. 8A). We chose 12 hours of additional light to maximize the response of the phase difference (See Fig. 8B). The pure populations and a 50:50 mixture of the mCherry and mVenus recorders were fluorescently detected every half hour over ten days simultaneously in the dark (D/D) (in Step 3). Cells were not isolated in oil droplets to allow communication. If there were no communication between cells, there would be no phase synchronization in the mixed population; however, if there were communication between cells, then there should be phase synchronization in the mixed

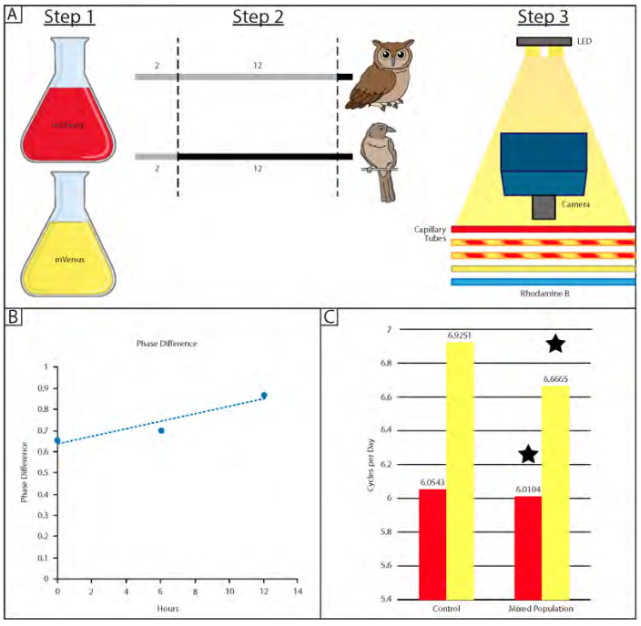

FIGURE 8. An equimolar mixture of mCherry (red) and mVenus (strains) converged in phase. (A) In Step 1 two strains were setup, one labeled with the mCherry recorder (in red) and one labeled with the mVenus recorder (in yellow). In Step 2 the mCherry received 12 hours more of light than the mVenus strain to become night owls. The time with the lights on is in grey, and the time when the lights are off is in black. In Step 3 five capillary tubes were loaded with three as controls. The capillary tube (in red) was loaded with a pure mCherry strain; the capillary tube (in yellow) was loaded with a pure mVenus strain. The capillary tube (in blue) was a third control loaded with Rhodamine B. The experimental capillary tubes with the equimolar mixtures of mCherry and mVenus strains are shown with candy stripes. At Step 3 all five tubes were imaged every half hour for ten days. (B) In order to document the shift of the light hours applied to the night owls in Step 3 a phase response in the difference between night owls and larks was constructed as a function of the shift in hours of the night owls. The difference in the phase [24](see Materials and Methods) was plotted against the phase shift in hours of light received. The Pearson correlation was $r = 0.9491$ ($P = 0.0001$) [53] and the Spearman rank correlation, $r_s = 1.00$ ($P = 0.3333$) [54]. The dashed line is a straight-line regression. (C) The mean phase for the pure and mixed cultures (measured in cycles per 24 h day) is shown for both mCherry and mVenus strains in bar charts. The differences between mean phase between the mVenus treatment (mixed culture) and mVenus controls (pure culture) and the mCherry strain vs. the mVenus strain in the mixed cultures were significantly different by an Analysis of Variance at the 0.01 level. Each mean in the bar chart was computed from over 12,000 cells. The standard errors about the sample means did not show up in this bar chart because they were so small. The stars indicate a significant difference between the mixed and pure cultures for the mVenus strain and the two mixed cultures.

population. The latter was observed with a decrease in the phase difference between the larks and night owls in the mixed population. The z-value of the comparison of the phase difference in the dark (D/D) between the pure and mixed cultures was $z = -665.92$ ($P < 0.00001$).

In this experiment the mVenus control strain (larks) is about.87 cycles per day faster than the mCherry control strain (night owls). Over ten days the phase of mVenus advanced about about 8.7 cycles relative to that of mCherry. In the same 10 day interval (24 h $\times$ 10) the mVenus pure control strain completed 69 cycles, but mCherry only completed 60 cycles. In contrast in the mixed population this phase

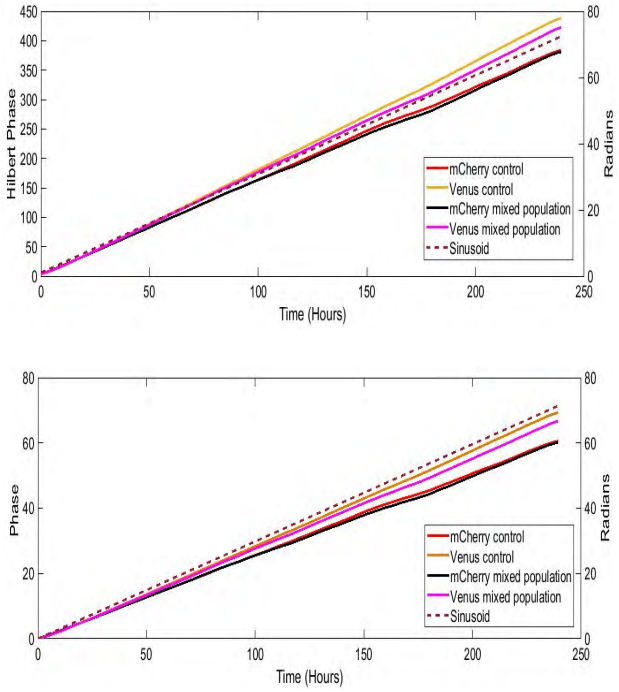

FIGURE 9. The average phase curves $M^C(t, 0)$ on over 48,000 cells supported phase synchronization emerging after 100 h when the mCherry (night owls) strain is given 12 h more of light than the mVenus (lark) strain before lights out D/D. In the top panel are the Hilbert Phase curves for the pure control strains and the mixed strain as well as the linear Hilbert phase curves (dotted line) $\omega t + \phi$ for a sinusoid Acos($\omega t + \phi$) as defined in the Results. All (i.e., mixed and control strains) sinusoid Hilbert phases were indistinguishable on the scale provided. In the bottom panel is the phase curve as defined in Materials and Methods and the Results as well as the phase ωt for the sinusoid. Again the phases for the sinusoids were collinear with each other for all strains. Phase was measured in cycles per ten days and is not divided by 10 as in Fig. 8 and S Fig. 13. Also the right scale reports the phases in radians for the sinusoid (dotted curve).

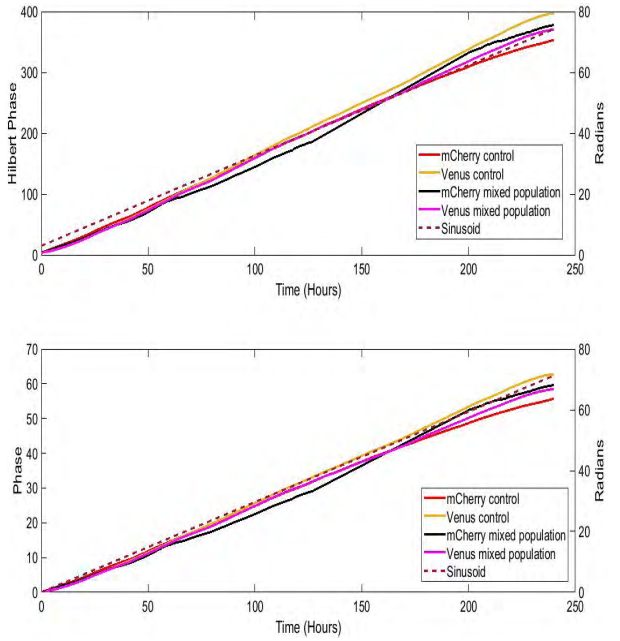

FIGURE 10. The average phase curves $M^C(t, 0)$ on over 46,000 cells supported phase synchronization emerging after 60 h when the mCherry (night owls) strain was given 6 h more of light than the mVenus (lark) strain before lights out D/D. In the top panel are the Hilbert Phase curves for the pure control strains and the mixed strain as well as the linear Hilbert phase curves (dotted line) $\omega t + \phi$ for a sinusoid Acos($\omega t + \phi$) as defined in the Materials and Methods. All (i.e., mixed and control strains) sinusoid Hilbert phases were indistinguishable on the scale provided. In the bottom panel is the phase curve as defined in Materials and Methods and the Results as well as the phase ωt for the sinusoid. Again the phases for the sinusoids were collinear with each other for all strains. Phase is measured in cycles per ten days and is not divided by 10 as in Fig. 8 and S Fig. 13. Also the right scale reports the phases in radians for the sinusoid (dotted curve).

difference shrank to 6.5 cycles per ten days (24 h × 10) or a phase difference of 0.65 per 24 h day. The advance in phase of mVenus of course depended on the time interval selected. In contrast the average periods from peaks in the periodograms were not very different with values ranging from 22 to 24 h by the periodograms of the mixed and control strains and 21 h from a fitted sinusoid (see Fig. 9 and 10 and S Fig. 11 and 12).

To examine the robustness of this finding, the experiment was perturbed with two changes. The microscope was upgraded to allow z-axis control in focusing to reduce the effects of focal-plane excursions by single cells, and the night owls only received 6 hours of additional light. The convergence was even more striking in the mixed culture (S Fig. 13) than that in Fig. 8C.

As a final control on these mixing experiments another 12 h shift experiment as in Fig. 8 was performed with the z-axis control (S Fig 14). Again in mixed cultures the final phase difference between night owls and larks was reduced at the end of the 10, 24 h day experiment relative to the pure cultures, after tracking 43,055 isolated cells over 10, 24 h days.

If the Hilbert phase or phase are considered as a function of time (t_1 varied from 0 to 10 24 h days) in Fig.s 9 and 10, then the initiation of phase synchronization can be observed after 12 h or 6 h of additional light for the night owls. In the experiment with 12 h light for the night owls synchronization began at ∼100 h in Fig. 9. mVenus cells from the mixed culture (pink) were seen to converge to mCherry cells, whether or not they were in a mixed or pure population. In the experiment with 6 h of additional light for the night owls synchronization began earlier at ∼60 h in Fig. 10. In this case both mVenus and mCherry cells from the mixed population were intermediate in phase between mVenus and mCherry cells from the pure populations.

It is useful to consider the Hilbert phase and phase for a sinusoid (dotted lines) in Fig.s 9 and 10, namely $\omega t + \phi$ and ωt. The phase shifts were all so small that mCherry and mVenus cells in pure and mixed cultures could not be distinguished in Fig.s 9 and 10. This highlights the danger of extrapolating from time 0 to 10, 24 h days from the phase shifts ϕ in S Fig.s 11 and 12. Even with this caveat the extrapolation surprisingly succeeded in S Fig. 11 for the experiment in which night owls receive an additional 12 h of light, but not for night owls that only receive 6 h of light

in S Fig. 12. By comparing the Hilbert Phase and Phase for a sinusoid to the same curves without this assumption, the reason why the linear extrapolation failed was seen. The average Hilbert and Phase curves constructed from the trajectories of 46,000-48,000 cells were nonlinear, implying that the periodic fluorescence of the cells are not sinusoidal, making a linear extrapolation challenging.

IV. DISCUSSION

Neurospora crassa and its relatives have long served as model systems for understanding a variety of biological processes [71] including the linkage of biochemistry and genetics [72], gene regulation [73], aging [74], [75], photobiology [76], epigenetics [77], and the clock [78]. It has also provided the context for the development of new omic and systems biology technologies including physical mapping [79], ensemble methods [80], MINE methods for model-guided discovery [36], [81], and large scale network reconstruction [25], [82]–[84]. Not surprisingly it will provide new insights into these fundamental processes by the development of new single cell technologies on conidial cells and single filaments.

The study of collective behavior [1], the emergence of interesting behaviors from the nonlinear interactions of living subsystems, in *N. crassa* is particularly facilitated by the ease of isolating single cells and filaments in this organism by microfluidics [85], [86]. This fact was exploited here to provide evidence that most individual conidial cells have intact clocks (Fig.s 2 and 7A). The studies here nicely complement temperature entrainment studies on *S. elongatus [16]* because light entrainment can be examined here easily in contrast to *S. elongatus*. (Fig. 2). Studies here also nicely complement those on mammalian tissue culture [17] because single *N. crassa* cells with intact biological clocks without neighbors can be isolated to examine the Stochastic Resonance hypothesis [20], a theory in which stochastic intracellular noise plays a positive role in single cell oscillations. Having established that single cells have clocks has also allowed us to examine common mechanisms of temperature compensation in a variety of clock systems (Fig. 7b) [45]. Similar approaches could be applied to other life stages, such as filaments, to understand the rules by which the organism forages for food, mates, ages, and adapts to a variable environment, such as the Light/Dark (L/D) cycle of the planet. How filaments extend themselves in their growth medium is organized and obeys certain rules, for example [87]. How the cells socialize [88] involves the interaction of cells that can be manipulated in a microfluidics device. How an organism ages can be examined directly as single cells age in different stressful environments [5].

The use of microfluidics technology here has provided an insight into the origins of the clock at the single cell level. We have found it unnecessary to postulate that the biological clock is an emergent property of cells communicating with each other; rather, here we provided evidence that each cell starts with an autonomously functioning biological clock (Fig. 2, S Fig. 3, and 7A). We have shown that there is substantial phase variation among the clocks of different cells (Fig.s 3-5). The challenge remains to understand how these cellular clocks synchronize phase at the macroscopic level in the face of substantial variation in phase between cellular clocks (Fig.s 3-5). We provided evidence here that cells do communicate phase information in the dark by mixing two cell populations completely out of phase, one being larks and one being night owls (Fig. 8 and S Fig. 13). The mixed population demonstrated convergence in phase and phase synchronization. On the other hand, Mihalescu *et al.* [12] have argued that such synchronization in single microbial cells could be attributed to shared causes of stochastic intracellular noise among cells. Recent experiments have shown the possibility of Stochastic Resonance between single cells that are isolated and in the dark [30]. Thus, both a communication hypothesis between autonomous single cell clocks and Stochastic Resonance remain viable hypotheses for explaining phase synchronization.

This phenomenon of phase synchronization is a form of collective behavior of cells, and a variety of theories (Fig. 6) are now being tested experimentally using microfluidics. We have provided evidence here that an external periodic driving signal of night and day (L/D) can serve to promote synchronization (Table 1), and we have also shown that when there is no such external driving signal present and cells are left in the dark (D/D), they phase-synchronized as well (Fig.s 8-10). This result may help to explain how cells do synchronize in the dark at the macroscopic scale in liquid culture or race tubes [5].

In this D/D situation one theory of phase synchronization involves a quorum sensing mechanism [89] that allows cells to synchronize through a shared signal in the medium or through cell to cell contact [24]. The individual oscillators could then set their clocks by virtue of a shared chemical signal. There is also now some initial evidence in the D/D experiments that there is a nonlinear relation between the level of shared periodicity of single cells and the stochastic intracellular noise within cells using models fitted to isolated single cells [30] that may contribute to phase synchronization. The effects of stochastic intracellular noise can be manipulated in single cell experiments to understand its role in generating synchronized diurnal rhythms at the macroscopic scale. A final theory of phase synchronization is through cell-cycle gated mechanisms of synchronization [14], [90]. Detailed models for how the clock works at the single cell level have been developed and will be tested at the single cell level by manipulating the environment of cells in a microfluidic environment [30].

V. CONCLUSION

The study of collective behavior is a compelling problem in biology [1]. The synchronization of clocks in single cells (as shown in Fig.s 2, 7, and 8) is a striking example of collective behavior. Several hypotheses have been advanced to explain collective behavior [1] by: 1) emergent properties

of nonlinear systems; 2) "follow the leader" behavior (*e.g.*, specific cells acting as cellular conductors of the orchestra of cellular clocks); 3) chemical sensing (*e.g.*, quorum sensing in the case of the clock [24]); 4) synchronization by noise under the Stochastic Resonance hypothesis [20]. Here we have provided evidence that the cells themselves have clocks (Fig. 2 and 7), and so a hypothesis based on emergent properties in an ensemble of cellular clocks to explain synchronization is unnecessary. Also the need for a cellular conductor as found in mammalian clocks [10] seems less likely since the evidence was that each *N. crassa* cell had its own autonomous clock (S Fig. 3). The challenge to understanding synchronization of cellular clocks in *N. crassa* under L/D conditions (Table 1) and D/D conditions [24] is the substantial noise at the single cell level (Fig.s 3- 5). Most of this stochastic intracellular noise manifested itself in variation in phase (Figs. 3-5). This suggests that clock communication may act through phase, prompting a need for a mixing experiment of two cellular clock populations out of phase. A quorum sensing model under the heading of chemical sensing and a positive role for stochastic intracellular variation under the Stochastic Resonance hypothesis appear to be strong candidates to explain the collective behavior of cellular clocks. For example, the quorum sensing model predicts phase synchronization (see supplementary video). To determine whether or not oscillators communicate phase information to synchronize their timekeeping, two mixing experiments were performed between two populations of clocks initially out of phase by 6 or 12 h. Under these two conditions the mixed population did phase synchronize (Fig. 8 and S Fig. 13). Our conclusion is that both the chemical sensing hypothesis of quorum sensing and the hypothesis of a positive role for stochastic intracellular noise under the Stochastic Resonance hypothesis [30] remain viable hypotheses in the light of the two mixing experiments in the microfluidic environment implemented here.

ACKNOWLEDGMENT

The funders had no role in study design, data collection and analysis, decision to publish, or preparation of the manuscript. *(Zhaojie Deng and Jia Hwei Cheong contributed equally to this work.)*

REFERENCES

[1] D. J. T. Sumpter, "The principles of collective animal behaviour," *Philos. Trans. Roy. Soc. B, Biol. Sci.*, vol. 361, no. 1465, pp. 5–22, 2005. doi: 10.1098/rstb.2005.1733.
[2] J. Buhl *et al.*, "From disorder to order in marching locusts," *Science*, vol. 312, pp. 1402–1406, Jun. 2006.
[3] A. Strandburg-Peshkin, D. R. Farine, I. D. Couzin, and M. C. Crofoot, "Shared decision-making drives collective movement in wild baboons," *Science*, vol. 348, no. 6241, pp. 1358–1361, 2015.
[4] M. Ballerini *et al.*, "Interaction ruling animal collective behavior depends on topological rather than metric distance: Evidence from a field study," *Proc. Nat. Acad. Sci. USA*, vol. 105, no. 4, pp. 1232–1237, 2008.
[5] M. Judge, J. Griffith, and J. Arnold, "Aging and the biological clock," in *Circadian Rhythms and Their Impact on Aging* (Healthy Aging and Longevity), S. M. Jazwinski, V. P. Belancio, S. M. Hill, and S. Rattan, Eds. Dordrecht, The Netherlands: Springer Science + Business Media, 2017, ch. 10, pp. 211–234.
[6] L. F. Larrondo, C. Olivares-Yañez, C. L. Baker, J. J. Loros, and J. C. Dunlap, "Decoupling circadian clock protein turnover from circadian period determination," *Science*, vol. 347, no. 6221, 2015, Art. no. 1257277.
[7] A. B. Webb, N. Angelo, J. E. Huettner, and E. D. Herzog, "Intrinsic, nondeterministic circadian rhythm generation in identified mammalian neurons," *Proc. Nat. Acad. Sci. USA*, vol. 106, no. 38, pp. 16493–16498, 2009.
[8] S. Yamaguchi *et al.*, "Synchronization of cellular clocks in the suprachiasmatic nucleus," *Science*, vol. 302, no. 5649, pp. 1408–1412, 2003.
[9] B. Grima, E. Chélot, R. Xia, and F. Rouyer, "Morning and evening peaks of activity rely on different clock neurons of the Drosophila brain," *Nature*, vol. 431, no. 7010, pp. 869–873, 2004.
[10] L. B. Duvall and P. H. Taghert, "The circadian neuropeptide PDF signals preferentially through a specific adenylate cyclase isoform AC3 in M pacemakers of Drosophila," *PLoS Biol.*, vol. 10, no. 6, 2012, Art. no. e1001337.
[11] G. De Palo, D. Yi, and R. G. Endres, "A critical-like collective state leads to long-range cell communication in Dictyostelium discoideum aggregation," *PLoS Biol.*, vol. 15, no. 4, 2017, Art. no. e1002602.
[12] I. Mihalcescu, W. Hsing, and S. Leibler, "Resilient circadian oscillator revealed in individual cyanobacteria," *Nature*, vol. 430, pp. 81–85, Jul. 2004.
[13] O. Mondragon-Palomino, T. Danino, J. Selimkhanov, L. Tsimring, and J. Hasty, "Entrainment of a population of synthetic genetic oscillators," *Science*, vol. 333, no. 6047, pp. 1315–1319, 2011.
[14] Q. Yang, B. F. Pando, G. Dong, S. S. Golden, and A. van Oudenaarden, "Circadian gating of the cell cycle revealed in single cyanobacterial cells," *Science*, vol. 327, no. 5972, pp. 1522–1526, 2010.
[15] M. Nakajima *et al.*, "Reconstitution of Circadian Oscillation of Cyanobacterial KaiC Phosphorylation in Vitro," *science*, vol. 308, no. 5720, pp. 414–415, 2005. doi: 10.1126/science.1108451.
[16] S. Gan and E. K. O'Shea, "An unstable singularity underlies stochastic phasing of the circadian clock in individual cyanobacterial cells," *Mol. Cell*, vol. 67, no. 4, pp. 659–672.e12, 2017.
[17] C. H. Ko *et al.*, "Emergence of noise-induced oscillations in the central circadian pacemaker," *PLoS Biol.*, vol. 8, no. 10, 2010, Art. no. e1000513.
[18] E. D. Buhr, S.-H. Yoo, and J. S. Takahashi, "Temperature as a universal resetting cue for mammalian circadian oscillators," *science*, vol. 330, no. 6002, pp. 379–385, 2010. doi: 10.1126/science.1195262.
[19] U. Abraham, A. E. Granada, P. O. Westermark, M. Heine, A. Kramer, and H. Herzel, "Coupling governs entrainment range of circadian clocks," *Mol. Syst. Biol.*, vol. 6, no. 1, p. 438, 2010. doi: 10.1038/msb.2010.92.
[20] R. Benzi, A. Sutera, and A. Vulpiani, "The mechanism of stochastic resonance," *J. Phys. A, Math. Gen.*, vol. 14, no. 11, p. L453, 1981.
[21] A. Gupta, B. Hepp, and M. Khammash, "Noise Induces the Population-Level Entrainment of Incoherent, Uncoupled Intracellular Oscillators," *Cell Syst.*, vol. 3, no. 6, pp. 521–531.e13, 2016.
[22] E. Ullner, J. Buceta, A. Díez-Noguera, and J. García-Ojalvo, "Noise-induced coherence in multicellular circadian clocks," *Biophys. J.*, vol. 96, no. 9, pp. 3573–3581, 2009.
[23] E. Castro-Longoria, M. Ferry, S. Bartnicki-Garcia, J. Hasty, and S. Brody, "Circadian rhythms in Neurospora crassa: Dynamics of the clock component frequency visualized using a fluorescent reporter," *Fungal Genet. Biol.*, vol. 47, no. 4, pp. 332–341, 2010.
[24] Z. Deng *et al.*, "Synchronizing stochastic circadian oscillators in single cells of *Neurospora crassa*," *Sci. Rep.*, vol. 6, Oct. 2016, Art. no. 35828.
[25] A. Al-Omari, J. Arnold, T. Taha, and H.-B. Schuttler, "Solving large nonlinear systems of first-order ordinary differential equations with hierarchical structure using multi-GPGPUs and an adaptive Runge Kutta ODE solver," *IEEE Access*, vol. 1, pp. 770–777, 2013.
[26] J. K. Brunson, J. Griffith, D. Bowles, M. E. Case, and J. Arnold, "lac-1 and lag-1 with ras-1 affect aging and the biological clock in *Neurospora crassa*," *Ecology Evol.*, vol. 6, no. 23, pp. 8341–8351, 2016.
[27] H. V. Colot *et al.*, "A high-throughput gene knockout procedure for Neurospora reveals functions for multiple transcription factors," *Proc. Nat. Acad. Sci. USA*, vol. 103, no. 27, pp. 10352–10357, Oct. 2006.
[28] D. D. Perkins, A. Radford, and M. S. Sachs, *The Neurospora Compendium : Chromosomal Loci*. New York, NY, USA: Academic, 2000.
[29] B. Hull, *Genomic Editing of Neurospora Crassa as A Tool for Studying Circadian Oscillator Synchronization*. Athens, GA, USA: University of Georgia, 2018.
[30] C. Caranica *et al.*, "Ensemble methods for stochastic networks with special reference to the biological clock of *Neurospora crassa*," *PLoS One*, vol. 13, no. 5, 2018, Art. no. e0196435.
[31] P. Thomas, A. V. Straube, J. Timmer, C. Fleck, and R. Grima, "Signatures of nonlinearity in single cell noise-induced oscillations," *J. Theor. Biol.*, vol. 335, pp. 222–234, Oct. 2013.

[32] L. Marple, "Computing the discrete-time 'analytic' signal via FFT," *IEEE Trans. Signal Process.*, vol. 47, no. 9, pp. 2600–2603, Sep. 1999.
[33] T. Kreuz, F. Mormann, R. G. Andrzejak, A. Kraskov, K. Lehnertz, and P. Grassberger, "Measuring synchronization in coupled model systems: A comparison of different approaches," *Phys. D, Nonlinear Phenomena*, vol. 225, no. 1, pp. 29–42, 2007.
[34] L. Lande-Diner, J. Stewart-Ornstein, C. J. Weitz, and G. Lahav, "Single-cell analysis of circadian dynamics in tissue explants," *Mol. Biol. Cell*, vol. 26, no. 22, pp. 3940–3945, 2015.
[35] T. Matsu-ura, M. Baek, J. Kwon, and C. I. Hong, "Efficient gene editing in *Neurospora crassa* with CRISPR technology," *Fungal Biol. Biotechnol.*, vol. 2, no. 1, p. 4, 2015.
[36] W. Dong *et al.*, "Systems biology of the clock in *Neurospora crassa*," *PLoS One*, vol. 3, no. 8, 2008, Art. no. e3105.
[37] M. Görl, M. Merrow, B. Huttner, J. Johnson, T. Roenneberg, and M. Brunner, "A PEST-like element in FREQUENCY determines the length of the circadian period in *Neurospora crassa*," *EMBO J.*, vol. 20, no. 24, pp. 7074–7084, Dec. 2001.
[38] A.-J. F. Carr and D. Whitmore, "Imaging of single light-responsive clock cells reveals fluctuating free-running periods," *Nature Cell Biol.*, vol. 7, pp. 319–321, 2005.
[39] T. Muranaka and T. Oyama, "Heterogeneity of cellular circadian clocks in intact plants and its correction under light-dark cycles," *Sci. Adv.*, vol. 2, no. 7, 2016, Art. no. e1600500. doi: 10.1126/sciadv.1600500.
[40] P. D. Gould *et al.*, "Coordination of robust single cell rhythms in the Arabidopsis circadian clock via spatial waves of gene expression," *Elife*, vol. 7, Apr. 2018, Art. no. e31700.
[41] B. Efron, "The Jacknife, the Bootstrap, and Other Resampling Plans," in *Proc. SIAM CBMS-NSF Regional Conf. Series Appl. Mathematics*, 1982, pp. 125–136.
[42] A. Arkin, J. Ross, and H. H. McAdams, "Stochastic kinetic analysis of developmental pathway bifurcation in phage λ-infected escherichia coli cells," *Genetics*, vol. 149, no. 4, pp. 1633–1648, 1998.
[43] L. Cai, C. K. Dalal, and M. B. Elowitz, "Frequency-modulated nuclear localization bursts coordinate gene regulation," *Nature*, vol. 455, no. 7212, pp. 485–490, 2008.
[44] Y. Lin, C. H. Sohn, C. K. Dalal, L. Cai, and M. B. Elowitz, "Combinatorial gene regulation by modulation of relative pulse timing," *Nature*, vol. 527, no. 7576, pp. 54–58, 2015.
[45] G. Kurosawa, A. Fujioka, S. Koinuma, A. Mochizuki, and Y. Shigeyoshi, "Temperature-amplitude coupling for stable biological rhythms at different temperatures," *PLoS Comput. Biol.*, vol. 13, no. 6, 2017, Art. no. e1005501.
[46] V. Bokka, A. Dey, and S. Sen, "Period–amplitude co-variation in biomolecular oscillators," *IET Syst. Biol.*, vol. 12, no. 4, pp. 190–198, 2018.
[47] C. Huygens, *Horologium Oscillatorium Sive De Motu Pendulorum*. Ames, IA, USA: Iowa State Univ. Press, 1673.
[48] H. M. Oliveira and L. V. Melo, "Huygens synchronization of two clocks," *Sci. Rep.*, vol. 5, p. 11548, Jul. 2015.
[49] D. Gabor, "Theory of communication. Part 1: The analysis of information," *J. Inst. Elect. Eng., Part III, Radio Commun. Eng.*, vol. 93, no. 26, pp. 429–441, Nov. 1946.
[50] A. T. Winfree, *The Geometry of Biological Time*. New York, NY, USA: Springer, 2001.
[51] T. Mojtaba Jafari *et al.*, "A real-time approach for heart rate monitoring using a Hilbert transform in seismocardiograms," *Physiolog. Meas.*, vol. 37, no. 11, pp. 1885–1909, 2016.
[52] J. K. Kim, "Protein sequestration versus Hill-type repression in circadian clock models," *IET Systems Biology*, vol. 10, no. 4, pp. 125–135, 2016.
[53] R. A. Fisher and F. Yates, *Statistical Tables for Biological, Agricultural and Medical Research*, 3rd ed. Essex, England: Longman, 1982, p. 64.
[54] M. Kendall and A. Stuart, *The Advanced Theory of Statistics: Inference and Relationship*, vol. 2. New York, NY, USA: Macmillan, 1979, p. 530.
[55] M. H. Vitaterna *et al.*, "The mouse Clock mutation reduces circadian pacemaker amplitude and enhances efficacy of resetting stimuli and phase–response curve amplitude," *Proc. Nat. Acad. Sci. USA*, vol. 103, no. 24, p. 9327, 2006. doi: 10.1073/pnas.0603601103.
[56] A. H. Chen, D. Lubkowicz, V. Yeong, R. L. Chang, and P. A. Silver, "Transplantability of a circadian clock to a noncircadian organism," *Sci. Adv., 10.1126/sciadv.1500358*, vol. 1, no. 5, 2015.
[57] M. Merrow, M. Brunner, and T. Roenneberg, "Assignment of circadian function for the *Neurospora* clock *gene frequency*," *Nature*, vol. 399, pp. 584–586, Jun. 1999.
[58] A. M. Pregueiro, N. Price-Lloyd, D. Bell-Pedersen, C. Heintzen, J. J. Loros, and J. C. Dunlap, "Assignment of an essential role for the Neurospora frequency gene in circadian entrainment to temperature cycles," *Proc. Nat. Acad. Sci. USA*, vol. 102, no. 6, p. 2210, 2005. doi: 10.1073/pnas.0406506102.
[59] Y. Yu *et al.*, "A genetic network for the clock of *Neurospora crassa*," *Proc. Nat. Acad. Sci. USA*, vol. 104, no. 8, pp. 2809–2814, Feb. 2007.
[60] Z. Deng, S. Arsenault, L. Mao, and J. Arnold, "Measuring synchronization of stochastic oscillators in biology," *J. Phys., Conf. Ser.*, vol. 750, no. 1, 2016, Art. no. 012001.
[61] S. Shinomoto and Y. Kuramoto, "Phase transitions in active rotator systems," *Prog. Theor. Phys.*, vol. 75, no. 5, pp. 1105–1110, 1986.
[62] C. S. Pittendrigh and D. H. Minis, "Circadian Systems: Longevity as a Function of Circadian Resonance in *Drosophila melanogaster*," *Proc. Nat. Acad. Sci. USA*, vol. 69, no. 6, pp. 1537–1539, Jun. 1972.
[63] N. Komin, A. C. Murza, E. Hernández-García, and R. Toral, "Synchronization and entrainment of coupled circadian oscillators," *Interface Focus*, vol. 1, no. 1, p. 167, 2011. doi: 10.1098/rsfs.2010.0327.
[64] C. S. Pittendrigh, "On temperature independence in the clock system controlling emergence in Drosophila," *Proc. Nat. Acad. Sci. USA*, vol. 40, no. 10, pp. 1018–1029, 1954.
[65] M. Zhou, J. K. Kim, G. W. L. Eng, D. B. Forger, and D. M. Virshup, "A period2 phosphoswitch regulates and temperature compensates circadian period," *Mol. Cell*, vol. 60, no. 1, pp. 77–88, 2015.
[66] Y. Liu, N. Y. Garceau, J. J. Loros, and J. C. Dunlap, "Thermally regulated translational control of FRQ mediates aspects of temperature responses in the neurospora circadian clock," *Cell*, vol. 89, no. 3, pp. 477–486, May 1997.
[67] X. Tang, "Computational systems biology for the biological clock of Neurospora crassa," Ph.D. dissertation, Dept. Phys. Astron., Univ. Georgia, Athens, GA, USA, 2009.
[68] A. Kalsbeek, S. L. Fleur, and E. Fliers, "Circadian control of glucose metabolism," *Mol. Metabolism*, vol. 3, no. 4, pp. 372–383, 2014.
[69] S. Y. Krishnaiah *et al.*, "Clock regulation of metabolites reveals coupling between transcription and metabolism," *Cell Metabolism*, vol. 25, no. 4, pp. 961–974, 2017.
[70] A. L. Cockrell *et al.*, "Suppressing the Neurospora crassa circadian clock while maintaining light responsiveness in continuous stirred tank reactors," *Sci. Rep.*, vol. 5, p. 10691, Jun. 2015.
[71] R. H. Davis, *Neurospora : Contributions of a Model Organism*. New York, NY, USA: Oxford Univ. Press, 2000.
[72] G. W. Beadle and E. L. Tatum, "Genetic control of biochemical reactions in neurospora," *Proc. Nat. Acad. Sci.USA*, vol. 27, no. 11, pp. 499–506, Nov. 1941.
[73] N. H. Giles *et al.*, "Gene organization and regulation in the qa (quinic acid) gene cluster of Neurospora crassa," *Microbiol. Rev.*, vol. 49, no. 3, pp. 338–358, Sep. 1985.
[74] H. Bertrand, A. J. F. Griffiths, and C. K. Cheng, "An extrachromosomal plasmid is the etiological precursor of kalDNA insertion sequences in the mitochrondrial chromosome of senescent neurospora," *Cell*, vol. 47, no. 5, pp. 829–837, 1986.
[75] C. Borghouts, E. Kimpel, and H. D. Osiewacz, "Mitochondrial DNA rearrangements of Podospora anserina are under the control of the nuclear gene grisea," *Proc. Nat. Acad. Sci. USA*, vol. 94, no. 20, pp. 10768–10773, 1997.
[76] L. Franchi, V. Fulci, and G. Macino, "Protein kinase C modulates light responses in *Neurospora* by regulating the blue light photoreceptor WC-1," *Mol. Microbiol.*, vol. 56, no. 2, pp. 334–345, Apr. 2005.
[77] E. U. Selker, "Premeiotic instability of repeated sequences in Neurospora crassa," *Annu. Rev. Genet.*, vol. 24, no. 1, pp. 579–613, 1990.
[78] J. C. Dunlap, "Molecular bases for circadian clocks," *Cell*, vol. 96, no. 2, pp. 271–290, Jan. 1999.
[79] J. Bennett and J. Arnold, "Genomics for fungi," in *Biology of the Fungal Cell*. Berlin, Germany: Springer, 2001, pp. 267–297.
[80] D. Battogtokh, D. K. Asch, M. E. Case, J. Arnold, and H.-B. Schüttler, "An ensemble method for identifying regulatory circuits with special reference to the qa gene cluster of *Neurospora crassa*," *Proc. Nat. Acad. Sci. USA*, vol. 99, no. 26, pp. 16904–16909, Dec. 2002.
[81] R. L. McGee and G. T. Buzzard, "Maximally informative next experiments for nonlinear models," *Math. Biosci.*, vol. 302, pp. 1–8, Aug. 2018.
[82] A. Al-Omari, J. Griffith, M. Judge, T. Taha, J. Arnold, and H.-B. Schüttler, "Discovering regulatory network topologies using ensemble methods on GPGPUs with special reference to the biological clock of Neurospora crassa," *IEEE Access*, vol. 3, pp. 27–42, 2015.

[83] A. Al-Omari, J. Griffith, C. Caranica, T. Taha, H.-B. Schüttler, and J. Arnold, "Discovering regulators in post-transcriptional control of the biological clock of Neurospora Crassausing variable topology ensemble methods on GPUS," *IEEE Access*, vol. 6, pp. 54582–54594, 2018.
[84] A. Al-Omari, H.-B. Schüttler, J. Arnold, and T. Taha, "Solving nonlinear systems of first order ordinary differential equations using a Galerkin finite element method," *IEEE Access*, vol. 1, pp. 408–417, 2013.
[85] K. K. Lee, L. Labiscsak, C. H. Ahn, and C. I. Hong, "Spiral-based microfluidic device for long-term time course imaging of *Neurospora crassa* with single nucleus resolution," *Fungal Genet. Biol.*, vol. 94, pp. 11–14, Sep. 2016.
[86] T. Geng *et al.*, "Compartmentalized microchannel array for high-throughput analysis of single cell polarized growth and dynamics," *Sci. Rep.*, vol. 5, Nov. 2015, Art. no. 16111.
[87] M. Held, C. Edwards, and D. V. Nicolau, "Probing the growth dynamics of *Neurospora crassa* with microfluidic structures," *Fungal Biol.*, vol. 115, no. 6, pp. 493–505, 2011.
[88] J. Heller, J. Zhao, G. Rosenfield, D. J. Kowbel, P. Gladieux, and N. L. Glass, "Characterization of greenbeard genes involved in long-distance kind discrimination in a microbial Eukaryote," *PLoS Biol.*, vol. 14, no. 4, 2016, Art. no. e1002431.
[89] D. A. Hogan, "Talking to themselves: Autoregulation and quorum sensing in fungi," *Eukaryotic Cell*, vol. 5, no. 4, pp. 613–619, 2006. doi: 10.1128/EC.5.4.613-619.2006.
[90] J. Paijmans, M. Bosman, P. R. T. Wolde, and D. K. Lubensky, "Discrete gene replication events drive coupling between the cell cycle and circadian clocks," *Proc. Nat. Acad. Sci. USA*, vol. 113, no. 15, pp. 4063–4068, 2015.

ZHAOJIE DENG received the B.S. and M.S. degrees in electrical and electronics engineering from the Huazhong University of Science and Technology, Wuhan, China, in 2008 and 2011, respectively, and the Ph.D. degree in biological and agricultural engineering from the University of Georgia, in 2017. She is currently a Staff Engineer with the Department of Genome Sciences, University of Washington. She has published over eight refereed publications on the microfluidics of single-cell measurements of the biological clock and of ferrofluids. Her research interests include the application of microfluidics and advanced imaging in genome sciences.

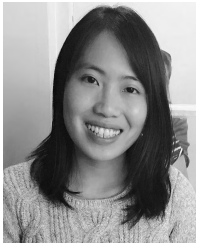

JIA HWEI CHEONG received the B.S. degree in chemistry from the University of Minnesota, in 2014. In 2016, she joined the University of Georgia as a Graduate Student in chemistry. Her research interest includes the circadian clock of the model systems, *Neurospora crassa*.

CRISTIAN CARANICA received the Ph.D. degree in mathematics from Louisiana State University, in 2009. He is currently pursuing the Ph.D. degree in statistics under the supervision of Prof. J. Arnold and Prof. H. B. Schuttler with the University of Georgia, Atlanta, GA, USA, with a focus on systems biology and stochastic genetic networks, where he is also a Research Assistant, under the NSF support, developing ensemble methods for stochastic networks. His current research interests include parallel computation, systems biology, stochastic biological circuits and gene networks, and inference about genetic networks with ensemble methods.

LINGYUN WU received the B.S. degree in physics from Portland State University, in 2012. He is currently pursuing the Ph.D. degree in physics with the University of Georgia. His research interests include the investigation of a hybrid model that combines stochastic gene regulation and deterministic time-evolution process of the circadian biological clock module in the bread mold, *Neurospora crassa*.

XIAO QIU received the B.S. degree in aircraft manufacturing engineering from Tongji University, China, in 2011, and the M.S. degree in fluid mechanics from Shanghai University, China, in 2015. In 2017, he joined the University of Georgia as a Graduate Student in bioinformatics. His research interests include systems biology, genetic networks, and single-cell circadian rhythms.

MICHAEL T. JUDGE received the B.Sc. degree in cell/molecular biology from Appalachian State University, Boone, NC, USA, with minors in mathematics and chemistry. He is currently pursuing the Ph.D. degree in genetics with the University of Georgia, Athens. His work has included gene editing and expression profiling, phenotyping and biochemical pathway dissection, and omics approaches and data analysis. He is currently developing *in vivo* methods for real-time monitoring of microbial metabolomes as well as open-source tools for metabolomics data analysis. He is a part of a long-term collaboration to leverage dynamic metabolomics data for a systems-level understanding of the *Neurospora crassa* metabolic network and circadian clock. His interests include metabolomics, systems/synthetic biology, metabolic engineering, data analysis/visualization, and science communication.

BROOKE HULL received the B.S. degree in genetics from the University of Georgia, in 2018. As a part of her B.S. degree in genetics, she completed an Honors Dissertation, which describes the engineering of a CRISPR/CAS9 mutant with mVenus recorder for the phase synchronization experiments. She is currently an NIH Postbaccalaureate Fellow with the Baylor College of Medicine.

CARMEN RODRIGUEZ received the M.S. degree in plant pathology from the University of Lisandro Alvarado, Barquisimeto, Venezuela, in 1992, and the Associate of Applied Science degree from the University of Los Andes, Venezuela, in 1983. From 1992 to 1995, she was a Research Mycologist with the Laboratory for Forest Products, Madison, WI, USA, under the supervision of Dr. H. Burdsall, Jr. In 2006, she became a Laboratory Manager II at the Genetics Department, University of Georgia, where she carried out research on epigenetics of plants and on circadian rhythms in the filamentous fungus, *Neurospora crassa*. She has over 35 years of research experience in fungal biology. In 1994, she became an Agricultural Research Coordinator under the supervision of Dr. R. Hanlin and Prof. C. Mims. She has published over six publications on the mycology and electron microscopy of plant pathogenic fungi.

JAMES GRIFFITH received the B.S. degree in animal and dairy science from the University of Georgia, in 1984. Following several years in the areas of bovine genetics, he joined the Genetics Department, University of Georgia, in 1989. He started out as a Research Technician and is currently the Lab Manager and a Research Professional for Dr. J. Arnold. He was heavily involved in the physical mapping of several fungi (*Aspergillus nidulans*, *Aspergillus flavus*, and *Neurospora crassa*) and for the last 11 years with longevity and the biological clock of *Neurospora crassa*. He has published over 20 publications on fungal genomics and systems biology.

AHMAD AL-OMARI received the B.Sc. degree in electrical and computer engineering from Yarmouk University, Irbid, Jordan, in 2004, and the Ph.D. degree in bioinformatics from the University of Georgia, Athens, GA, USA, in 2015. He then joined the Department of Biomedical Systems and Bioinformatics Engineering, College of Engineering, Yarmouk University, where he currently serves as a Professor of bioinformatics. He is also an Erasmus+ CBHE Grant Proposal Trainer. He is considered as the first Bioinformatician in Jordan. He has many published papers and posters in bioinformatics, numerical methods, and parallel algorithms on the GPGPUs. His research interests include parallel computation, systems biology, numerical analysis, biological circuits, and gene networks. He received grants from different institutes to pursue his research, including NVIDIA.

SAM ARSENAULT received the bachelor's degrees in mathematics and biology with a focus on neuroscience from the University of Georgia, where he is currently pursuing the Ph.D. degree with the Department of Entomology, under the guidance of Dr. B. Hunt. His Ph.D. thesis was on Exploring the Genetic and Epigenetic Basis for Social Polymorphisms in Hymenoptera. He worked with Dr. J. Arnold at the Department of Genetics and Dr. L. Mao at the College of Engineering on the computational modeling of circadian rhythms in the fungus, *Neurospora crassa*. His research interest includes exploring the genetic regulation of queen number in the red imported fire ant, *Solenopsis invicta*.

HEINZ-BERND SCHÜTTLER received the Diploma degree in physics from Technische Universität München, Germany, in 1981, and the Ph.D. degree in physics from the University of California at Los Angeles, in 1984. After postdoctoral appointments at the University of California at Santa Barbara and the Argonne National Laboratory, he joined the faculty of the Department of Physics and Astronomy, University of Georgia, in 1987, where he currently serves as a Professor of physics. His research interests include applications of computational statistical mechanics in biology and condensed matter physics. His recent notable contributions in computational biology include the development of the ensemble network simulation (ENS) method for the reconstruction of biological circuits and the ENS-based methods for maximally informative next experiment (MINE) design.

LEIDONG MAO received the B.S. degree in materials science from Fudan University, Shanghai, China, in 2001, and the M.S. and Ph.D. degrees in electrical engineering from Yale University, New Haven, CT, USA, in 2002 and 2007, respectively. He is currently a Full Professor with the College of Engineering, University of Georgia, USA. His current research interests include microfluidic technologies for circulating-tumor-cell and single-cell research. He has secured more than $3.1 million in funding. His research efforts have resulted in over 29 peer-reviewed journal papers, three granted U.S. patents, and 12 invited presentations (six international). His research program has been recognized by the Young Scientist Award of the International Society of Magnetic Fluids, in 2013, the UGA Distinguished Faculty Fellow Award, in 2016, and the Lab on a Chip Emerging Investigator, in 2017.

JONATHAN ARNOLD received the B.S. degree in mathematics and the M.Phil. and Ph.D. degrees in statistics from Yale University, in 1975, 1978, and 1982, respectively. In 1982, he joined the Departments of Statistics and Genetics, College of Arts and Sciences, University of Georgia, where he has risen through the ranks to Professor of genetics, statistics, and physics and astronomy. He has authored or coauthored over 140 papers in journals, book chapters, and conference proceedings in the fields of statistical genetics, population genetics, computational biology, fungal genomics, and systems biology. His research interests include the development and identification of genetic networks of fundamental processes in the model systems, *Neurospora crassa*, i.e., computing life. He was elected as an AAAS Fellow, in 2011. He has served as a Charter Member on the NIH Genetic Variation and Evolution Study Section. He has served on the NSF Computational Biology Panel, the DOE Genome Panel, and the NSF Systems and Synthetic Biology Panel.